NASA Contractor Report 191555
ICASE Report No. 93-78

ICASE

20 Years of Excellence

SHAPE OPTIMIZATION GOVERNED BY THE EULER EQUATIONS USING AN ADJOINT METHOD

Angelo Iollo
Manuel D. Salas
Shlomo Ta'asan

NASA Contract No. NAS1-19480
November 1993

Institute for Computer Applications in Science and Engineering
NASA Langley Research Center
Hampton, Virginia 23681-0001

Operated by the Universities Space Research Association

National Aeronautics and
Space Administration

Langley Research Center
Hampton, Virginia 23681-0001

SHAPE OPTIMIZATION GOVERNED BY THE EULER EQUATIONS USING AN ADJOINT METHOD

Angelo Iollo[1]
Dipartimento di Ingegneria Aeronautica e Spaziale, Politecnico di Torino
Institute for Computer Applications in Science and Engineering

Manuel D. Salas
NASA Langley Research Center

Shlomo Ta'asan[2]
The Weizman Institute of Science
Institute for Computer Applications in Science and Engineering

ABSTRACT

In this paper we discuss a numerical approach for the treatment of optimal shape problems governed by the Euler equations. In particular, we focus on flows with embedded shocks. We consider a very simple problem: the design of a quasi-one-dimensional Laval nozzle. We introduce a cost function and a set of Lagrange multipliers to achieve the minimum. The nature of the resulting costate equations is discussed. A theoretical difficulty that arises for cases with embedded shocks is pointed out and solved. Finally, some results are given to illustrate the effectiveness of the method.

[1]This research was supported in part under NASA Contract No. NAS1-19480, while the first author was in residence at the Institute for Computer Application in Science and Engineering, NASA Langley Research Center, Hampton, VA 23681.

[2]This research was supported in part under the Incumbent of the Lilian and George Lyttle Career Development Chair, and in part under NASA Contract No. NAS1-19480, while the third author was in residence at the Institute for Computer Application in Science and Engineering, NASA Langley Research Center, Hampton, VA 23681.

1 Introduction

The physical structure of the complex flows that occur in aerodynamic design can be predicted by reliable numerical simulations. On the other hand, the increasing capability of computers to perform even larger calculations radically changes the aerodynamic design process. Indeed, for engineering purposes, if one can predict performance, it is fundamental to know which modification of an aerodynamic configuration improves performance.

This question has, of course, been addressed long before the advent of computers which has led to a broad category of methods known as inverse design. An exhaustive account of the historical development of these approaches is given in [1]. Here it is suffice to say that these methods, pioneered by Lighthill [6], require knowledge of a desirable pressure or velocity distribution. The adequacy of the distribution chosen is dependent on the experience of the designer; the resulting shape strongly depends on this choice. An original example of such an approach is found in [3]

The numerical approach that we will use in this paper, lift the dependence on heuristic choices of the desirable distribution, allowing the imposition of constrains to be satisfied by the solution found. The numerical simulation of the flow and a numerical optimization code are coupled. The optimization code calculates the best perturbation to the geometry to decrease a cost function. The geometry itself is described by a set of shape coefficients.

The optimization code can be devised in one of several ways. A common approach is to perturb one shape coefficient at a time and compute the derivative of the cost function with respect to this coefficient as a finite difference. Although such codes are simple to devise, the procedure is costly and can introduce large errors. In a further evolution of this approach, an equation is first calculated for the derivative of the cost function with respect to the shape coefficient and then solved numerically. An equation must be solved for each shape coefficient. A recent application of this method to a two-dimensional supersonic problem is found in [2].

The approach presented in this paper is a classical optimal control method. We will introduce costate variables (Lagrange multiplier) to achieve a minimum. This method has been successfully applied in the design of an airfoil in a subsonic potential flow [10].

Here, we consider a flow with embedded shocks where the governing equations are the Euler equations. We show how to derive an analytical expression of the cost function derivatives with respect to the shape coefficients. For this purpose, we solve only one set of costate equations. In [9], some difficulties are outlined, and a method to avoid them is proposed. In the present approach an optimal shape can be found for problems with embedded shocks, without additional complications. A careful examination of the structure of the costate equations suggests a method for integrating them with a robust algorithm developed for fluid dynamics purposes.

A comparison of optimization-based approaches for aerodynamics design problems is given in [7], although some results for flows with embedded shocks have been questioned recently in [9].

2 Problem Statement

We investigate a new method for aerodynamic design and optimization based on the Euler equations. In order to demonstrate the ideas of the method, a very simple problem is considered: the design of a Laval nozzle assuming inviscid, quasi-one-dimensional flow. The optimization problem consists of finding a set of design variables (in this case shape parameters) that minimize some cost function, e.g., a desired pressure or velocity distribution along the centerline and possibly requiring that some side constraints be satisfied. We attack the optimization problem with the adjoint method. The adjoint method introduces a new set of equations and unknowns that are solved together with the flow-field equations. To better understand how to obtain a solution of the adjoint equations, the properties of these equations are discussed.

Let the extension of the Laval nozzle in physical space be $\Omega = [0, l]$. An energylike functional denoted by $\mathcal{E}$, is the cost function we want to satisfy. An optimal shape of the nozzle is reached when we meet the necessary conditions for a minimum of $\mathcal{E}$. Let

$$\mathcal{E} = \frac{1}{2}\int_0^l (p - p^*)^2 dx$$

where p^* is a target pressure distribution along the abscissa x and p is the pressure field for the present geometry. The choice of the functional does not affect the generality of the method once the dependence of $\mathcal{E}$ with respect to the flow-field variables is determined. Nevertheless, the choice of the functional itself (e.g., $|p - p^*|$ instead of $(p - p^*)^2$) can affect the performance of the optimization algorithm by changing the curvature of the energylike surface.

In the case of a quasi-one-dimensional flow, if we denote

$$\begin{aligned}
\rho &= \text{density} \\
u &= \text{velocity} \\
e &= \text{specific total energy} \\
p &= \text{pressure} \\
a &= \text{speed of sound} \\
h &= \text{height of the channel} \\
\gamma &= \text{specific heat ratio} \\
\kappa &= \frac{\gamma - 1}{2}
\end{aligned}$$

then the Euler equations for unsteady flows reduce to

$$\mathbf{U}_t + \mathbf{F}_x + \mathbf{Q} = \mathbf{0} \tag{1}$$

where

$$\mathbf{U} = \begin{pmatrix} \rho \\ \rho u \\ \rho e \end{pmatrix} \quad \mathbf{F} = \begin{pmatrix} \rho u \\ p + \rho u^2 \\ u(\rho e + p) \end{pmatrix} \quad \mathbf{Q} = \begin{pmatrix} \rho u \beta \\ \rho u^2 \beta \\ u(\rho e + p)\beta \end{pmatrix}$$

$\beta = h_x/h$, and $p = \kappa\rho(2e - u^2)$. In the following derivation, we use the homogeneity property

$$\mathbf{F} = \mathbf{A}(\mathbf{U})\mathbf{U} \tag{2}$$

where

$$\frac{\partial \mathbf{F}}{\partial \mathbf{U}} = \mathbf{A}(\mathbf{U}) \tag{3}$$

and

$$\mathbf{A}(\mathbf{U}) = \begin{pmatrix} 0 & 1 & 0 \\ \frac{1}{2}(\gamma-3)u^2 & (3-\gamma)u & 2\kappa \\ 2\kappa u^3 - \gamma ue/p & \gamma e/p - 3\kappa u^2 & \gamma u \end{pmatrix}$$

The source term $\mathbf{Q}$ can be written to display its dependence on $\mathbf{U}$; in fact, the multiplication can be carried out to show that

$$\mathbf{Q} = \mathbf{S}(\mathbf{U})\mathbf{U} \tag{4}$$

where

$$\mathbf{S}(\mathbf{U}) = \frac{\partial \mathbf{Q}}{\partial \mathbf{U}} = \beta \begin{pmatrix} 0 & 1 & 0 \\ -u^2 & 2u & 0 \\ 2\kappa u^3 - \gamma ue/p & \gamma e/p - 3\kappa u^2 & \gamma u \end{pmatrix} \tag{5}$$

The first and the third row of $\mathbf{A}(\mathbf{U})$ are proportional to the first and third row of $\mathbf{S}(\mathbf{U})$, respectively . Furthermore because $d(\rho u^2) = -u^2 \cdot d\rho + 2u \cdot d(\rho u)$ and $\rho u^2 = -u^2 \cdot \rho + 2u \cdot \rho u$, it follows that $\mathbf{S}(\mathbf{U}) = \partial \mathbf{Q}/\partial \mathbf{U}$.

We refer to the solution of the above equations as the analysis problem. The boundary conditions for this problem must be chosen such that the problem is well posed. In particular, we will consider the inlet flow with a constant total pressure and entropy, i.e., $p^o_{in} = p_{in}(1 + \kappa M^2_{in})^{\gamma/\gamma-1} = \text{Constant}$, $p_{in}/\rho^{\gamma}_{in} = \text{Constant}$. At the outlet, if the flow is subsonic, the static pressure is fixed as $p_{out} = \text{Constant}$.

3 Adjoint Formulation for a Shockless Case

The design problem can be thought of as a search for a minimum of a functional under constrains. Let

$$\mathcal{L}(\alpha_i) = \mathcal{E} + \int_{\Omega} \mathbf{\Lambda}^T(\mathbf{F}_x + \mathbf{Q})dx \tag{6}$$

where $\mathbf{\Lambda}^T$ is an arbitrary vector with components $(\lambda_1(x), \lambda_2(x), \lambda_3(x))$, Ω is the domain $[0, l]$, and α_i are shape coefficients that define the geometry of the nozzle, for example by $h(\alpha_i, x) = \sum_i \alpha_i f_i(x)$ with $f_i(x)$ a generic function of x. Since in the steady state the Euler equations must be satisfied everywhere in the domain, the functionals $\mathcal{E}$ and $\mathcal{L}$ are identical. If we increase the shape coefficients by $\varepsilon\widetilde{\alpha_i}$, then the latter functional will change by an amount, say, $\varepsilon\delta\mathcal{L}$. The other quantities will change in the same way: $\beta \Rightarrow \beta + \varepsilon\widetilde{\beta}$, $p \Rightarrow p + \varepsilon\widetilde{p}$, and $\mathbf{U}(x) \Rightarrow \mathbf{U}(x) + \varepsilon\widetilde{\mathbf{U}}(x)$, where $\widetilde{\mathbf{U}} = (\widetilde{\rho}, \widetilde{\rho u}, \widetilde{\rho e})^T$. By using eqs.(3) and

(5), we obtain also $\mathbf{F}(x) \Rightarrow \mathbf{F}(x) + \varepsilon \mathbf{A}(\mathbf{U})\widetilde{\mathbf{U}}(x)$ and $\mathbf{Q}(x) \Rightarrow \mathbf{Q}(x) + \varepsilon \mathbf{S}(\mathbf{U})\widetilde{\mathbf{U}}(x)$. If we substitute these relations into eq.(6) and retain only the first-order terms, we obtain

$$\delta\mathcal{L} = \int_0^l \widetilde{p}(p - p^*)dx + \int_0^l \mathbf{\Lambda}^T\{[\mathbf{A}(\mathbf{U})\widetilde{\mathbf{U}}]_x + \mathbf{S}(\mathbf{U})\widetilde{\mathbf{U}}\}dx + \int_0^l \frac{\widetilde{\beta}\mathbf{\Lambda}^T\mathbf{S}(\mathbf{U})\mathbf{U}}{\beta}dx \qquad (7)$$

In the above equation, $\widetilde{\beta} = (\widetilde{h}_x h - \widetilde{h}h_x)/h^2$. With the notation $c_i(x) = (hf_{i_x} - h_x f_i)/h^2$, the last integral of eq.(7) can be written as

$$\sum_i \widetilde{\alpha}_i \int_0^l \frac{c_i \mathbf{\Lambda}^T \mathbf{S}(\mathbf{U})\mathbf{U}}{\beta}dx \qquad (8)$$

in which the substitution $\widetilde{\beta} = \sum_i \widetilde{\alpha}_i c_i$ is made.

Let us integrate by parts the second integral in eq.(7), with $\mathbf{A} = \mathbf{A}(\mathbf{U})$ and $\mathbf{S} = \mathbf{S}(\mathbf{U})$ we obtain

$$\int_0^l \mathbf{\Lambda}^T[(\mathbf{A}\widetilde{\mathbf{U}})_x + \mathbf{S}\widetilde{\mathbf{U}}]dx = [\mathbf{\Lambda}^T\mathbf{A}\widetilde{\mathbf{U}}]_0^l - \int_0^l \mathbf{\Lambda}_x^T\mathbf{A}\widetilde{\mathbf{U}}dx + \int_0^l \mathbf{\Lambda}^T\mathbf{S}\widetilde{\mathbf{U}}dx \qquad (9)$$

The first term on the right-hand side of the above equation drops for a suitable choice of $\mathbf{\Lambda}$ at the boundaries. The boundary conditions for $\widetilde{\mathbf{U}}$ are complementary to those for $\mathbf{\Lambda}$, in the sense that $\mathbf{\Lambda}^T\mathbf{A}\widetilde{\mathbf{U}} = 0$ yields a homogeneous linear system in $\mathbf{\Lambda}$ whose rank depends on the number of boundary conditions for $\widetilde{\mathbf{U}}$.

For this test case, at the inlet we have

$$p_{in}^o = \text{Constant}$$

which implies that

$$\widetilde{p} = -\rho u \widetilde{u}$$

If the entropy is fixed, then the specific total enthalpy is also constant; therefore,

$$\frac{\gamma p}{(\gamma - 1)\rho} + \frac{1}{2}u^2 = \text{Constant}$$

We conclude that

$$[\mathbf{A}\widetilde{\mathbf{U}}]_0 = [\widetilde{\rho u}, u\widetilde{\rho u}, (\frac{\gamma p}{(\gamma - 1)\rho} + \frac{1}{2}u^2)\widetilde{\rho u}]^T$$

Hence, the suitable choice at the inlet for $\mathbf{\Lambda}$ is

$$\lambda_1 + u\lambda_2 + \left[\frac{\gamma p}{(\gamma - 1)\rho} + \frac{1}{2}u^2\right]\lambda_3 = 0 \qquad (10)$$

At the outlet for a subsonic case with a given p_{out}, we obtain

$$[\mathbf{A}\widetilde{\mathbf{U}}]_l = \{\widetilde{\rho u}, 2u\widetilde{\rho u} - u^2\widetilde{\rho}, \left[\frac{\gamma p}{(\gamma - 1)\rho} + \frac{3}{2}u^2\right]\widetilde{\rho u} - u\left[\frac{\gamma p}{(\gamma - 1)\rho} + u^2\right]\widetilde{\rho}\}^T$$

which leads to

$$\begin{aligned} \lambda_1 + 2u\lambda_2 + \left[\frac{\gamma p}{(\gamma-1)\rho} + \frac{3}{2}u^2\right]\lambda_3 &= 0 \\ u\lambda_2 + \left[\frac{\gamma p}{(\gamma-1)\rho} + u^2\right]\lambda_3 &= 0 \end{aligned} \tag{11}$$

If the outflow is supersonic, then no boundary conditions are required for $\widetilde{\mathbf{U}}$; therefore,

$$\mathbf{\Lambda} = 0 \tag{12}$$

identically at the outlet.

If we take boundary conditions (10) and (11) and eq.(9) into account, eq.(7) can be rewritten as

$$\delta\mathcal{L} = \int_0^l \widetilde{\mathbf{U}}^T[-\mathbf{A}^T\mathbf{\Lambda}_x + \mathbf{S}^T\mathbf{\Lambda} + \frac{\partial p}{\partial \mathbf{U}}(p-p^*)]dx + \sum_i \tilde{\alpha}_i \int_0^l \frac{c_i \mathbf{\Lambda}^T \mathbf{S}\mathbf{U}}{\beta} dx \tag{13}$$

where $\partial p/\partial \mathbf{U} = \frac{\gamma-1}{2}(u^2, -2u, 2)$. If we select $\mathbf{\Lambda}$ such that

$$-\mathbf{A}^T\mathbf{\Lambda}_x + \mathbf{S}^T\mathbf{\Lambda} + \frac{\partial p}{\partial \mathbf{U}}(p-p^*) = 0 \tag{14}$$

eq.(13) becomes

$$\delta\mathcal{L} = \sum_i \frac{\partial \mathcal{L}}{\partial \alpha_i}\tilde{\alpha}_i = \sum_i \tilde{\alpha}_i \int_0^l \frac{c_i \mathbf{\Lambda}^T \mathbf{S}\mathbf{U}}{\beta} dx$$

in which we recognize

$$\frac{\partial \mathcal{L}}{\partial \alpha_i} = \int_0^l \frac{c_i \mathbf{\Lambda}^T \mathbf{S}\mathbf{U}}{\beta} dx \tag{15}$$

Suppose that the flow field is known, such that all the variables, dependent upon $\mathbf{U}$, are fixed. If we solve eq.(14) with the appropriate boundary conditions for $\mathbf{\Lambda}$ and substitute the results in eq.(15), then we obtain a formulation for the gradient of the Lagrangian. The problem then is reduced to finding the solution of a linear system of equations in $\mathbf{\Lambda}$ with homogeneous boundary conditions. Note that $\mathbf{\Lambda} = \mathbf{0}$ is a solution if $p = p^*$, which is a sufficient condition for $\delta\mathcal{L} = 0$. If at the minimum $p \neq p^*$ although the integral in eq.(15) is 0, then in general $\mathbf{\Lambda} \neq \mathbf{0}$. The discussion thus far leads to some basic questions about the well posedness of the eq.(14) with the boundary conditions given by eqs.(10), (11) or (12) and about the existence and uniqueness of the solution. To actually determine a solution of this system, examine eq.(14), embedded in time as

$$\pm\,\mathbf{\Lambda}_t - \mathbf{A}^T\mathbf{\Lambda}_x + \mathbf{S}^T\mathbf{\Lambda} + \frac{\partial p}{\partial \mathbf{U}}(p-p^*) = 0 \tag{16}$$

in which we must choose for the proper sign for the time derivative.

The matrix $\mathbf{A}^T$ has the familiar eigenvalues $u-a$, u and $u+a$. At the boundaries, if we choose the positive sign in eq.(16), for each boundary condition there will be an incoming characteristic, such that the problem is well posed. Another motivation for this choice is that if we add to eq.(1) the diffusive term, when integrated by parts twice, it would append to eq.(14) a second derivative term in x with the same sign this term had in the flow equations. Therefore, if the negative sign in eq.(16) is adopted, then an ill-posed heat equation would result. In conclusion, note that the costate equation

$$\mathbf{\Lambda}_t - \mathbf{A}^T\mathbf{\Lambda}_x + \mathbf{S}^T\mathbf{\Lambda} + \frac{\partial p}{\partial \mathbf{U}}(p-p^*) = 0 \tag{17}$$

has an upside-down characteristic pattern with respect to the time-dependent flow equation. If we consider a transonic nozzle, in the throat area, the eigenvalue $u-a$ goes continuously through zero; the flow undergoes an expansion through a transonic fan. On the other hand, the behavior of the same family of characteristics for eq.(17) shows a shocklike pattern. The two characteristic patterns are illustrated in figs.1(a) and 1(b).

For a reason that will be clear later, some ambiguous jump conditions for this shock will be derived. First consider a simple equation of the kind $\Phi_t - x\Phi_x = 0$, with $\Phi = \Phi(x)$, $x \in [-1,1]$, and boundary conditions $\Phi(-1) = \Phi_l$, $\Phi(1) = \Phi_r$. The characteristics at the boundaries show that this problem is well posed and independent of the initial conditions, for a large t, the solution will be a step function $\Phi(x) = \Phi_l$ for $x \in [-1,0[$ and $\Phi(x) = \Phi_r$ for $x \in]0,1]$. Note that the jump at zero is solely determined by the boundary conditions and that the steady solution will be reached for $t \to \infty$ because of the nearly vertical characteristics next to $x = 0$.

The structure of the solution to this equation is similar to that underlying eq.(17) for which the analysis hides somehow this behavior. A solution to eq.(14) can be written in the form

$$\mathbf{\Lambda}(x) = \mathcal{C}(x) + [\mathbf{\Lambda}]H(x - x_{th})$$

where $\mathcal{C}(x) \in C^1$, $[\mathbf{\Lambda}]$ is the jump at the shock, $H(x-x_{th})$ is the Heaviside function, and x_{th} is the location of the shock for $\mathbf{\Lambda}$ (i.e., the throat of the nozzle). If we substitute in eq.(14), because $\delta(x)$ (which is the Dirac measure of x) is the derivative of $H(x)$ with respect to x, we obtain at $x = x_{th}$

$$\mathbf{A}^T[\mathbf{\Lambda}]\delta(x - x_{th}) = 0$$

in which all the negligible terms have been dropped. Note that the presence of source terms in eq.(14) does not affect the derivation of the jump conditions.

Finally, because at $x = x_{th}$ $\det \mathbf{A} = 0$, we obtain a nontrivial solution for the system

$$\mathbf{A}^T[\mathbf{\Lambda}] = \mathbf{0} \tag{18}$$

which yields only two jump conditions; the third jump condition depends on the boundary conditions. In this sense this problem has ambiguous jump conditions.

If the only solution of the homogeneous problem associated with eq.(14), i.e.

$$-\mathbf{A}^T\mathbf{\Lambda}_x + \mathbf{S}^T\mathbf{\Lambda} = 0 \tag{19}$$

and its boundary conditions, is $\mathbf{\Lambda} = \mathbf{0}$, then the solution with a nonhomogeneous source term is unique, since eq.(14) is linear. Let us consider a subsonic case, with det $\mathbf{A} \neq 0$ everywhere in the domain. A general solution of eq.(19) can be written as

$$\mathbf{\Lambda} = \mathbf{\Lambda}_0 e^{\int_0^l (\mathbf{A}^T)^{-1}\mathbf{S}^T dx}$$

and, together with boundary conditions (10) and (11), this implies $\mathbf{\Lambda} = 0$ on the domain. In the transonic case, since det$\mathbf{A} = 0$ at $x = x_{th}$, we split the problem into two domains, such that in the subsets $[0, x_{th}[$ and $]x_{th}, l]$, det$\mathbf{A} \neq 0$. The solution will be

$$\mathbf{\Lambda}_{sub} = \mathbf{\Lambda}'_0 e^{\int_0^{x_{th}} (\mathbf{A}^T)^{-1}\mathbf{S}^T dx} \text{ for } x \in [0, x_{th}[$$

and

$$\mathbf{\Lambda}_{super} = \mathbf{\Lambda}''_0 e^{\int_{x_{th}}^l (\mathbf{A}^T)^{-1}\mathbf{S}^T dx} \text{ for } x \in]x_{th}, l].$$

Again, if we account for the inlet boundary conditions (10), the jump conditions from eq.(18), and the outlet boundary conditions (12), then the solution is $\mathbf{\Lambda} = 0$.

In summary, we have derived an analytic formulation for the gradient of the Lagrangian in eq.(6) with respect to the geometry. Furthermore, we have shown that this representation is unique in the sense discussed above.

4 Costate Equations for a Shock Case

Until now, we have limited our investigation to shockless nozzles to avoid certain difficulties that we will discuss here. One problem is that eq.(1) and, therefore, eq.(16) are not defined at the shock. This problem is overcome by extending the solution space of $\mathbf{U}(x)$ to a set of generalized functions, such that eq.(1) will reduce to the Rankine-Hugoniot jumps at the shock. A more subtle shortcoming is better understood with the aid the following example. Consider a simple equation of the kind $\Phi_t + (H(x) - 1/2)\Phi_x = 0$ that is defined, for example, on $\Omega = [-1, 1]$. The characteristics pattern (fig.2), shows the necessity of some boundary conditions on both sides of the the discontinuity to ensure the existence of a steady-state solution, regardless of the boundary conditions at the ends of the domain Ω.

Now, eq.(17) can be rewritten to reflect its characteristics pattern

$$\mathbf{P}^T\mathbf{\Lambda}_t - \mathbf{D}\mathbf{P}^T\mathbf{\Lambda}_x + \mathbf{P}^T\mathbf{S}^T\mathbf{\Lambda} + \mathbf{P}^T\frac{\partial p}{\partial \mathbf{U}}(p - p^*) = 0 \tag{20}$$

where

$$\mathbf{P} = \begin{pmatrix} 1 & 1 & 1 \\ u - a & u & u + a \\ (e + p) - ua & \frac{1}{2}u^2 & (e + p) + ua \end{pmatrix}$$

is the matrix of the right eigenvectors of $\mathbf{A}(\mathbf{U})$, and

$$\mathbf{D} = \begin{pmatrix} u-a & 0 & 0 \\ 0 & u & 0 \\ 0 & 0 & u+a \end{pmatrix}$$

At the shock wave, the characteristic that corresponds to the eigenvalue $u-a$ undergoes a jump in speed of the kind described in the example. If this point is considered inside the domain of calculation, then some condition is needed to update the solution in time. A boundary condition is needed at this point to continue the calculation to the left of the shock wave. We cannot try to derive some boundary conditions for this point, as explained for the inlet and the outlet. No speculation about the perturbation $\widetilde{\mathbf{U}}$ at the shock is possible because a perturbation that is solely dependent on the shape coefficients α_i and the flow equations would be chosen arbitrarily. No other constrains exist. For example, the application of the Rankine-Hugoniot jumps to $\widetilde{\mathbf{U}}$ on each side of the shock would be equivalent to assuming that the shock does not change position regardless of the value of $\widetilde{\alpha_i}$. The integrals in eq.(7) are split in two, and the integration is carried between $[0, x_{sh}[$ and $]x_{sh}, l]$ as

$$\delta\mathcal{L} = \delta\mathcal{L}_1 + \delta\mathcal{L}_2,$$

where

$$\begin{aligned} \delta\mathcal{L}_1 &= [\mathbf{\Lambda}^T\mathbf{A}\widetilde{\mathbf{U}}]_0^{x_{sh}} + \int_0^{x_{sh}} \widetilde{\mathbf{U}}^T[-\mathbf{A}^T\mathbf{\Lambda}_x + \mathbf{S}^T\mathbf{\Lambda} + \frac{\partial p}{\partial \mathbf{U}}(p-p^*)]dx \\ &\quad + \sum_i \widetilde{\alpha}_i \int_0^{x_{sh}} \frac{c_i\mathbf{\Lambda}^T\mathbf{S}\mathbf{U}}{\beta}dx \end{aligned} \tag{21}$$

and

$$\begin{aligned} \delta\mathcal{L}_2 &= [\mathbf{\Lambda}^T\mathbf{A}\widetilde{\mathbf{U}}]_{x_{sh}}^{l} + \int_{x_{sh}}^{l} \widetilde{\mathbf{U}}^T(-\mathbf{A}^T\mathbf{\Lambda}_x + \mathbf{S}^T\mathbf{\Lambda} + \frac{\partial p}{\partial \mathbf{U}}(p-p^*))dx \\ &\quad + \sum_i \widetilde{\alpha}_i \int_{x_{sh}}^{l} \frac{c_i\mathbf{\Lambda}^T\mathbf{S}\mathbf{U}}{\beta}dx \end{aligned} \tag{22}$$

A suitable choice for the Lagrange multiplier is to take $\mathbf{\Lambda} = 0$ on both sides of the shock such that $\mathbf{\Lambda}$ is continuous. This selection frees us from imposing a condition on $\widetilde{\mathbf{U}}$, because the addendum $[\mathbf{\Lambda}^T\mathbf{A}\widetilde{\mathbf{U}}]$ in eqs.(21) and (22) drops anyway at the shock. At the shock, we will have three characteristics that deliver the information $\mathbf{\Lambda} = 0$ to the left domain, and one that delivers it to the right.

We have examined also another possible interpretation of eqs.(21) and (22). Assume that for some perturbation of the shape coefficients α_i, the shock properties do not change, i.e., the jump in total pressure across it, is essentially constant, which will be the case for a weak shock. If we assume that the total enthalpy is constant, then the field to pa:formulationthe right of the shock can be regarded as a subsonic nozzle governed by eq.(17) with boundary conditions (10) and (11). To the left of the shock, the flow behaves

as a supersonic outlet, where we must impose the proper boundary condition, eq.(12), as discussed earlier. With this approach, $\delta\mathcal{L}_1 = 0$ and $\delta\mathcal{L}_2 = 0$ independently at the minimum.

The two approaches presented to handle the shock are not significantly different. In the numerical calculations that follow, we have implemented the second set of boundary conditions.

5 Numerical Approach

The flow-field solution is obtained by introducing a discrete grid $(x_n, t_k) = (x_0 + n\Delta x, t_0 + \sum_k \Delta t_k)$, where Δx is constant and Δt_k changes to satisfy the CFL condition. The conservative variables $\mathbf{U}(x)$ are computed at the cell centers and integrated in time with a three-stage Runge-Kutta scheme, as explained in [5]. In this implementation, we interpolate $\mathbf{U}(x)$ to the cell faces by using characteristic differences and a minmod limiter. The flux derivative in eq.(1) is then computed using an approximate Riemann solver. See [4]. Away from discontinuities, the scheme is second order accurate.

Depending on the case considered, the solutions of the costate eq.(14), are sought as steady results of eq.(17), with boundary conditions applied as explained in the previous section. Although eq.(17) is linear, it presents some numerical difficulties because of the characteristics pattern at the throat and at the shock location. In particular, consider eq.(20) discretized over the same uniform grid of the analysis problem with spacing Δx. If we denote by $\Delta(\cdot)^v$ the finite increments of the function $(\cdot)$ with respect to the superscripted variable, we have, at each grid point

$$\mathbf{P}^T \frac{\Delta \mathbf{\Lambda}^t}{\Delta t} - \mathbf{D}\mathbf{P}^T \frac{\Delta \mathbf{\Lambda}^x}{\Delta x} + \mathbf{P}^T \mathbf{S}^T \mathbf{\Lambda} + \mathbf{P}^T \frac{\partial p}{\partial \mathbf{U}}(p - p^*) = 0 \tag{23}$$

Define the local increment $\Delta \mathbf{W} = \mathbf{P}^T \Delta \mathbf{\Lambda}$; with this notation eq.(23) becomes

$$\frac{\Delta \mathbf{W}^t}{\Delta t} - \mathbf{D}\frac{\Delta \mathbf{W}^x}{\Delta x} + \mathbf{P}^T \mathbf{S}^T \mathbf{\Lambda} + \mathbf{P}^T \frac{\partial p}{\partial \mathbf{U}}(p - p^*) = 0. \tag{24}$$

This equation describes the signals that propagate along the characteristics; therefore, the increment $\Delta \mathbf{W}^x$, is one-sided depending on the sign of the corresponding propagation speed. Note that for this equation it would be impossible to use a conservative scheme since no conservation law exists to satisfy. The integration in time is made by explicit time stepping. The scheme is first-order accurate.

At the throat of the nozzle, $u - a = 0$ and $\beta = 0$; hence, the first row of eq.(24) reduces to

$$\frac{\Delta \mathbf{W}^t}{\Delta t} + \mathbf{P}^T \frac{\partial p}{\partial \mathbf{U}}(p - p^*) = 0$$

The eigenvalue $u - a$ has been shown to vanish at the throat. For a grid point in the neighborhood of the throat, this singularity can lead to unbounded grows for Lambda, depending on the nature of the source term in the above equation. Because the other two

characteristics are nonzero at the throat, this error can degrade the entire calculation. To avoid this problem, we approximate $u - a$ with its value at the neighboring point on the side from which the vanishing characteristic propagates.

Since with a Godunov-type solver the shock is resolved with three grid points, we must decide on which of these to impose the boundary conditions for $\mathbf{\Lambda}$. We must consider that the middle point of the three cells on which the shock is solved, is almost sonic; if the boundary conditions for $\mathbf{\Lambda}$ at a subsonic inlet (eq.(10)) were imposed at this grid point, then the convergence rate to the steady solution would be considerably slower. For this reason we impose the condition for supersonic outlet $\mathbf{\Lambda} = 0$, on the middle grid point, eliminating it from of the computation.

Another remark should be made in regard to the order of magnitude of the residuals of eq.(23), for which we can consider the solution steady. Close to the minimum, the gradients in eq.(15) are almost zero; nevertheless the optimization algorithm requires a careful computation of these values, such that in order to consider the time-dependent solution converged, the residuals must be some orders of magnitude smaller than the gradient components.

In the results that follow, we used a representation of the nozzle geometry defined by $h = \alpha_1 X + \alpha_2/X + \alpha_3$, where $X = x + 10^{-3}$; this representation allows two independent design variables because $\beta = h_x/h$.

In this work, we do not address the methods to accelerate the numerical scheme to obtain an optimal shape; the strategy used to achieve the minimum of the functional is straightforward:

1. Start with a first guess for the shape coefficients.
2. Solve the flow equation.
3. Solve the costate equation with the values computed in step 2 for the flow field.
4. Update the shape coefficient with a gradient-based criterion.
5. Restart the procedure from step 2 until the gradient is zero.

To update the shape coefficients a BFGS algorithm was used. See [8]. In some cases, as we will discuss, we used an inefficient, but robust, algorithm that simply makes a line search for a zero of the gradient.

6 Discussion of the Results and Conclusions

The values for the functional $\mathcal{E}$, computed with an analytical solution of eq.(1), are shown in fig.(3). The numerical values of the analytical solution are computed on the same grid presented above; then, the functional is computed by a trapezoidal approximation. The discrete functional, which is a result of the trapezoidal integration, shows some discontinuities and a local minimum that disappears as the number of grid points increases. As

the mesh is refined, the number of the discontinuities increases, while the jumps become smaller.

Note that if the dependence of the geometry on the shape coefficients is smooth, then the functional

$$\frac{\partial \mathcal{E}}{\partial \alpha_i} = \int_\Omega \frac{\partial p}{\partial \alpha_i}(p - p^*)dx$$

is always defined with the assumption that $\partial p/\partial \alpha_i$ is defined everywhere except at a finite number of points. This assumption is reasonable because the solution of eq.(1) changes smoothly with the geometry. For this reason, even if no certainty exists that the solution depends monotonically on the shape coefficients, this behavior can be the interpreted in this way. Suppose that the integrand of the functional can be represented by a simple rectangular function. If in attaining the minimum the area under the curve decreases and its "height" increases, the functional will eventually increase before the edges of the rectangle pass another grid point, because the mesh resolution is not sufficient. The functional will exhibit a local minimum and a subsequent discontinuity.

A method that derives a formulation for the gradient of $\mathcal{E}$ from a discrete approximation of the functional will obtain meaningless solutions as a result of the discontinuities of the discrete functional, such that no optimization algorithm alone could anyway get to the minimum. In the present formulation, an approximate representation of the analytical gradient of the functional is derived. For this reason, the approximation of the analytical gradient will be, at most, affected by discontinuities due to the discretization and will be always monotonic (if the analytical functional does not change curvature) and bounded. See fig.4. In figs.5 and 6, we present two sets of results in which the target pressure distribution was generated with the same $h(x)$ that was used in the optimization procedure. In fig.5, the target pressure distribution is obtained starting from a subsonic first guess. This result shows the effectiveness of the method. Fig.6 shows that we can achieve the optimum from both sides of the discontinuity.

In general, when $p^*(x)$ is fixed, the minimum of $\mathcal{E}$ is reached for different values of the shape coefficient α_i. These different values depend on whether one considers the analytical or the discretized functional, even if the results are converged on the grid. If the target solution can be attained exactly, then both values coincide. The gradient calculated after the proposed derivation, will still depend on the discretization through the nonhomogeneous term in eq.(14). In fig.7, we show, for a case in which p^* cannot be reached exactly, that the distance between the two minima becomes approximately half when the grid resolution is doubled. This result supports the hypothesis that the minimum calculated through the analytical gradient will indefinitely approach to the actual minimum as the grid is refined.

In conclusion, a method has been presented to calculate the gradient components of a generic functional, in which (regardless of the number of the shape coefficients) only one linear costate equation must be solved. The minimum computed in this way differs from the minimum of the discrete functional; however these minima indefinitely approach as the grid is refined.

References

[1] Jameson A. Aerodynamic design via control theory. Technical Report 88-64, ICASE, 1988.

[2] Borggaard J., Burns J.A. Cliff E., and Gunzburger M. Sensitivity calculations for a 2d, inviscid, supersonic forebody problem. Technical Report 93-13, ICASE, 1993.

[3] Zannetti L. A natural formulation for the solution of two-dimensional or axisymmetric inverse problems. *Int. J. Numerical Methods in Engineering*, vol.22:451–463, 1986.

[4] Pandolfi M. On the flux-difference splitting formulation. *Notes on Numerical Fluid Mechanics*, vol.26, 1989. Vieweg Verlag.

[5] Salas M.D. Shock wave interaction with an abrupt area change. Technical Report TP 3113, NASA, 1991.

[6] Lighthill M.J. A new method of two dimensional aerodynamic design. *ARC Rand M 2112*, 1945.

[7] Frank P.D. and Shubin G.R. A comparison of optimization-based approaches for a model computational aerodynamics design problem. *J. Computational Physics*, vol.98:74–89, 1992.

[8] Fletcher R. *Practical Methods of Optimization*, volume 1. John Wiley & Sons, 1980.

[9] Narducci R., Grossman B., and Haftka R.T. Design sensitivity algorithms for an inverse design problem involving a shock wave. Submitted to the AIAA 32nd Aerospace Sciences Meeting, Jan. 1994.

[10] Ta'asan S., Kuruvila G., and Salas M.D. Aerodynamic design and optimization in one shot. In *30th Aerospace Sciences Meeting and Exibit, AIAA 92-005*, Jan. 1992.

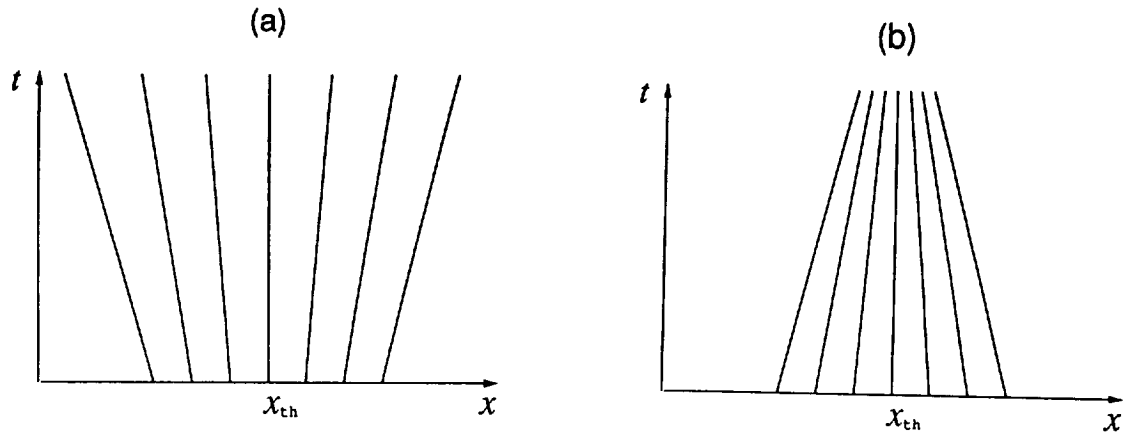

Figure 1: Characteristic patterns. (a) Transonic expansion. (b) Correspondent shocklike structure for costate equations.

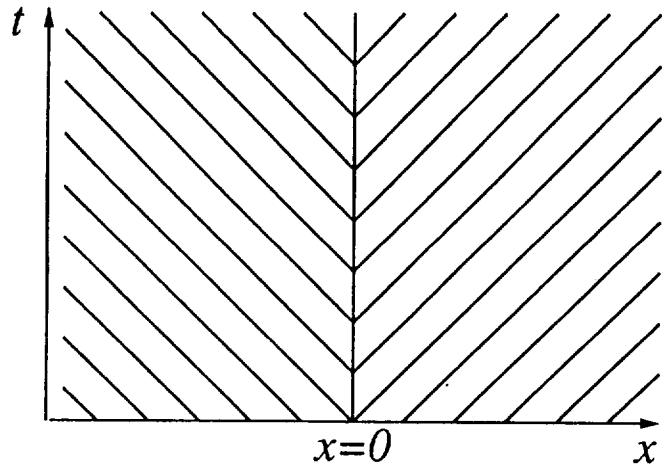

Figure 2: Characteristic pattern for $\Phi_t + [H(x) - 1/2]\Phi_x = 0$. Boundary conditions are needed on both sides of discontinuity.

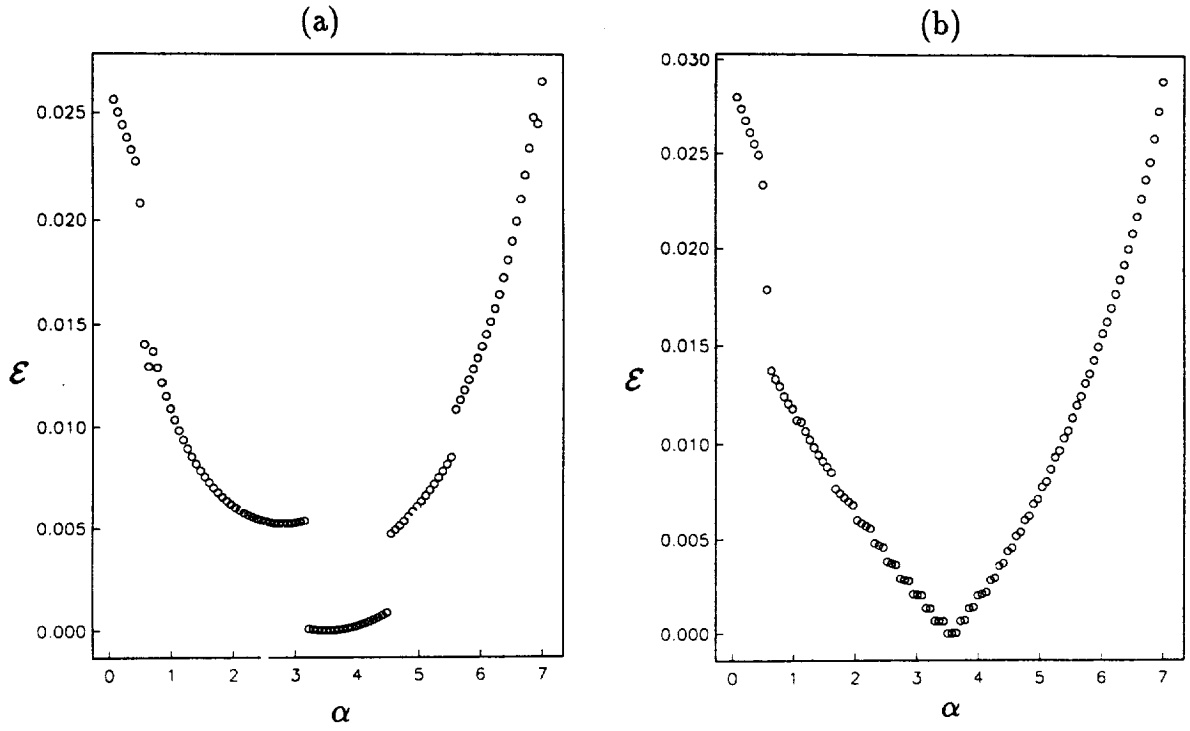

Figure 3: Analytical solution calculated with shape function $h(x) = \alpha(x^3 - x^2) + 1.05$; functional has been calculated with trapezoidal approximation. (a) Solution distributed over 20 grid points. (b) Solution distributed over 80 grid points.

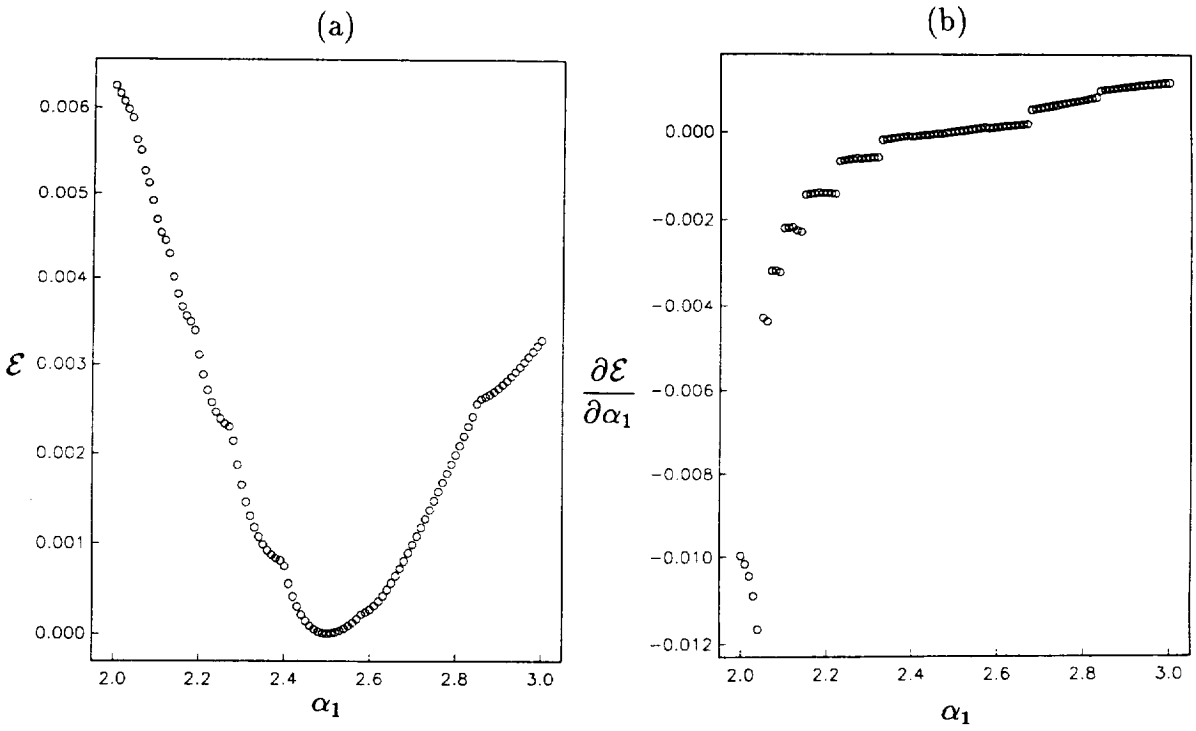

Figure 4: Result shown is obtained with $h(x) = \alpha_1 X + 0.3/X + 10$. For each value of α_1 flow equation is solved by a Godunov like scheme, and gradient is calculated as proposed in this paper. Each time the shock goes through grid point, discretized functional does not have a monotonic derivative; gradient has discontinuities, but is still monotonic. (a) Functional. (b) Gradient.

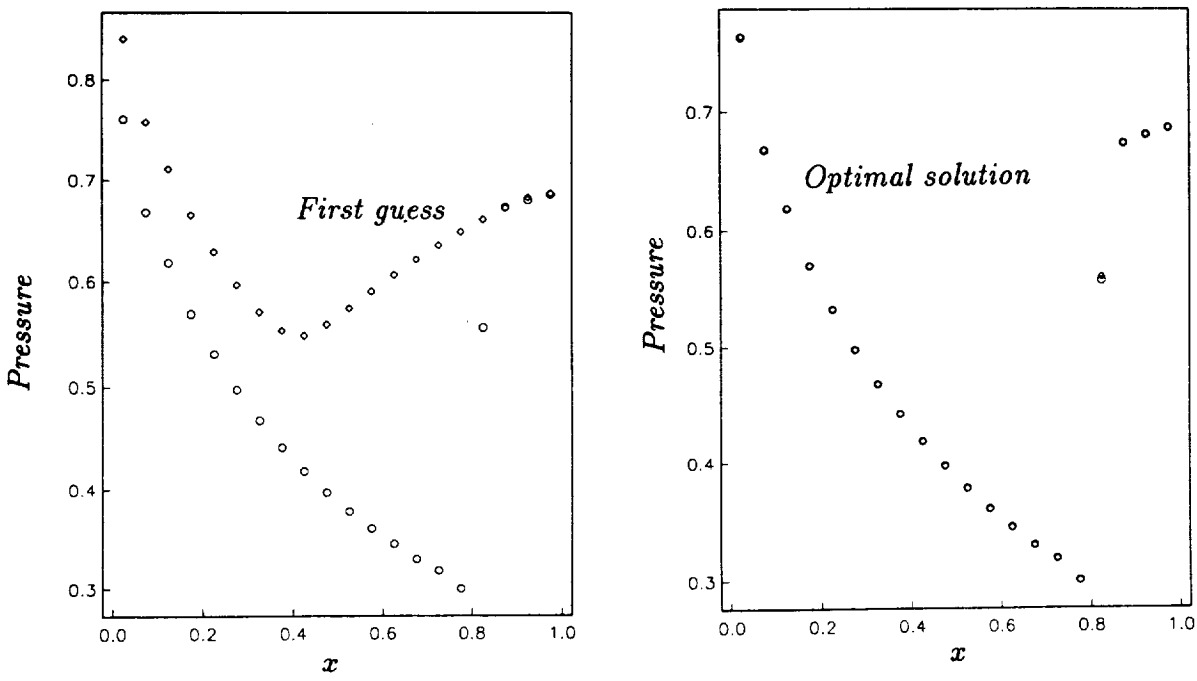

Figure 5: Target solution is $h(x) = 2.5X + 0.3/X + 5$. First guess is $h(x) = 2X + 0.52/X + 5$. Shape function for which minimum is sought is $h(x) = \alpha_1 X + \alpha_2/X + 5$, and optimization algorithm used is BFGS. Starting value of the functional is of order 10^{-3}. At minimum it is of order 10^{-9}. Gradient components are of order 10^{-12} at minimum.

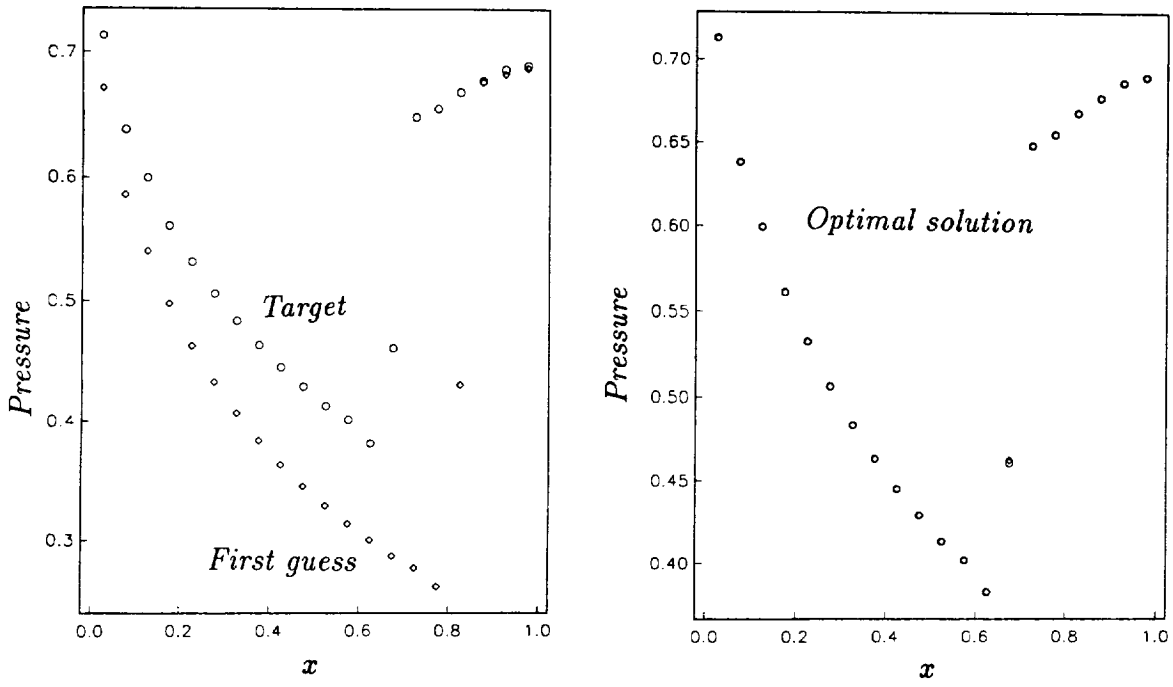

Figure 6: Target solution is $h(x) = 2.5X+0.3/X+10$. First guess is $h(x) = 5X+0.3/X+10$. Shape function for which minimum is sought is $h(x) = \alpha_1 X + \alpha_2/X + 10$, and optimization algorithm used is BFGS. Starting value of functional is of order of 10^{-3}. At minimum it is of order 10^{-9}. Gradient components are of order 10^{-12} at minimum.

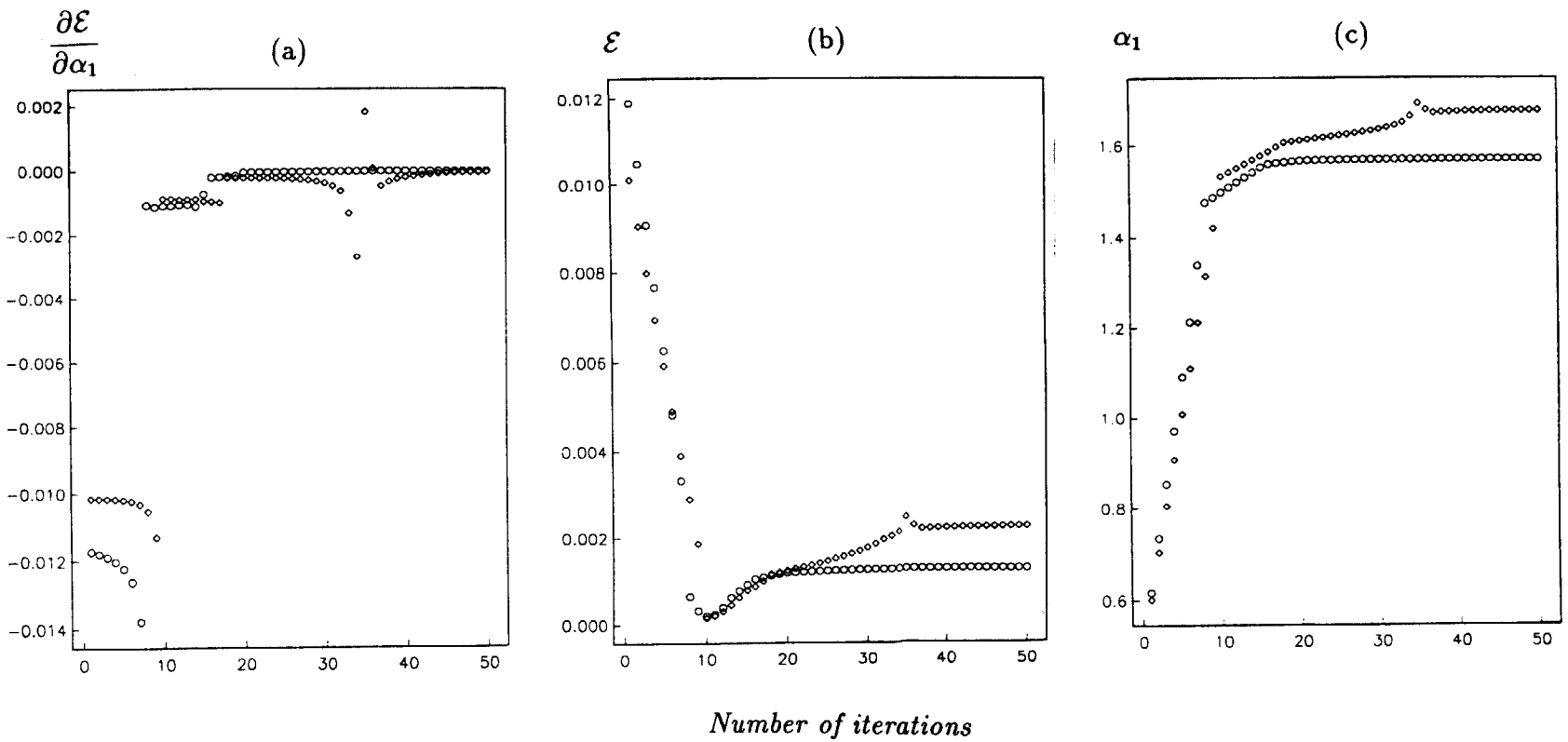

Figure 7: Target solution is $h(x) = 2.5X + 0.4/X + 10$, and the shape function for which minimum is sought is $h(x) = \alpha_1 X + 0.3/X + 5$. Divide and conquer procedure was used to find zero of gradient. (a) Convergence of gradient to zero. (b) Functional value, at zero of gradient, is reduced to half by doubling grid points. (c) Design variable.

REPORT DOCUMENTATION PAGE

Form Approved
OMB No. 0704-0188

1. AGENCY USE ONLY(Leave blank)	2. REPORT DATE	3. REPORT TYPE AND DATES COVERED
	November 1993	Contractor Report

4. TITLE AND SUBTITLE
SHAPE OPTIMIZATION GOVERNED BY THE EULER EQUATIONS USING AN ADJOINT METHOD

5. FUNDING NUMBERS
C NAS1-19480
WU 505-90-52-01

6. AUTHOR(S)
Angelo Iollo
Manuel D. Salas
Shlomo Ta'asan

7. PERFORMING ORGANIZATION NAME(S) AND ADDRESS(ES)
Institute for Computer Applications in Science
and Engineering
Mail Stop 132C, NASA Langley Research Center
Hampton, VA 23681-0001

8. PERFORMING ORGANIZATION REPORT NUMBER
ICASE Report No. 93-78

9. SPONSORING/MONITORING AGENCY NAME(S) AND ADDRESS(ES)
National Aeronautics and Space Administration
Langley Research Center
Hampton, VA 23681-0001

10. SPONSORING/MONITORING AGENCY REPORT NUMBER
NASA CR-191555
ICASE Report No. 93-78

11. SUPPLEMENTARY NOTES
Langley Technical Monitor: Michael F. Card
Final Report
To be submitted to "14th Int'l Conf. on Num. Meth. in Fluid Dyn.", July 11-15, 1994, Bangalore, India

12a. DISTRIBUTION/AVAILABILITY STATEMENT
Unclassified–Unlimited

Subject Category 64

12b. DISTRIBUTION CODE

13. ABSTRACT *(Maximum 200 words)*

In this paper we discuss a numerical approach for the treatment of optimal shape problems governed by the Euler equations. In particular, we focus on flows with embedded shocks. We consider a very simple problem: the design of a quasi-one-dimensional Laval nozzle. We introduce a cost function and a set of Lagrange multipliers to achieve the minimum. The nature of the resulting costate equations is discussed. A theoretical difficulty that arises for cases with embedded shocks is pointed out and solved. Finally, some results are given to illustrate the effectiveness of the method.

14. SUBJECT TERMS	15. NUMBER OF PAGES
optimal shape; adjoint; shocks	20
	16. PRICE CODE A03

17. SECURITY CLASSIFICATION OF REPORT	18. SECURITY CLASSIFICATION OF THIS PAGE	19. SECURITY CLASSIFICATION OF ABSTRACT	20. LIMITATION OF ABSTRACT
Unclassified	Unclassified		

NSN 7540-01-280-5500

Standard Form 298(Rev. 2-89)
Prescribed by ANSI Std. Z39-18
298-102

☆U.S. GOVERNMENT PRINTING OFFICE: 1993 - 528-064/86089